



POLITECNICO DI TORINO  
Repository ISTITUZIONALE

Black-Box Modeling of the Maximum Currents Induced in Harnesses During Automotive Radiated Immunity Tests

*Original*

Black-Box Modeling of the Maximum Currents Induced in Harnesses During Automotive Radiated Immunity Tests / Trincherò, Riccardo; Stievano, Igor S.; Canavero, Flavio G.. - In: IEEE TRANSACTIONS ON ELECTROMAGNETIC COMPATIBILITY. - ISSN 0018-9375. - ELETTRONICO. - 62:2(2019), pp. 627-630.

*Availability:*

This version is available at: 11583/2768140 since: 2020-04-20T10:27:07Z

*Publisher:*

IEEE

*Published*

DOI:10.1109/TEM.2019.2903270

*Terms of use:*

openAccess

This article is made available under terms and conditions as specified in the corresponding bibliographic description in the repository

*Publisher copyright*

ieee

copyright 20xx IEEE. Personal use of this material is permitted. Permission from IEEE must be obtained for all other uses, in any current or future media, including reprinting/republishing this material for advertising or promotional purposes, creating .

(Article begins on next page)

# Black-Box Modeling of the Maximum Currents Induced in Harnesses During Automotive Radiated Immunity Tests

Riccardo Trincherò, *Member, IEEE*, Igor S. Stievano, *Senior Member, IEEE*, Flavio G. Canavero, *Fellow, IEEE*

**Abstract**—This paper presents a black-box modeling approach for the prediction of the spectrum of the maximum currents induced on a generic linear load in an automotive radiated immunity test. The proposed approach relies on a parametric Thévenin-based circuit equivalent built from a limited set of measured or simulated data. The frequency-domain behavior of the equivalent voltage source is provided via a metamodel by combining the support vector machine (SVM) regression with a regularized Fourier kernel with a simple adaptive algorithm. The latter allows defining the minimum number of training samples needed to accurately predict the maximum values of the currents induced on a generic linear load for different azimuth directions of the excitation field. The accuracy and the strength of the proposed modeling are demonstrated for an example, by comparing the model predictions with the results of a parametric full-wave electromagnetic simulation.

**Index Terms**—Automotive EMC, radiated immunity test, metamodel, support vector machine, numerical simulation.

## I. INTRODUCTION

The growing demand for additional functionalities and features in automotive vehicles leads to an increasing integration of on-board electrical and electronic devices. Typical examples are represented by electronic control units (ECUs), actuators, and sensors which are massively used in modern vehicles and behave as both sources and victims of radiated and conducted electromagnetic interferences (EMI) [1]–[2].

Within the electromagnetic compatibility (EMC) scenario, the effects of the external fields on the most relevant part of the electronic systems is investigated via the radiated immunity test [3]–[4]. The above test consists in irradiating a vehicle placed on a rotating platform in a large anechoic chamber with an external electromagnetic (EM) field. The measured currents, produced by the external field on the electronic components of interest, are required to comply with the maximum levels imposed by EMC standards [5]. It is important to remark that several simulations or measurements with different angular positions of the vehicle are required in order to guarantee an accurate prediction of the maximum current spectrum, leading to a non-negligible cost in terms of either computational time or measurement overhead.

Therefore, an accurate model of the complex physical phenomena involved in the radio frequency (RF) immunity assessment turns out to be a valuable resource allowing the

EMC engineers to estimate the induced current profiles for different design scenarios (e.g., for different sizes of the cable shields [7]) and to assess the benefits of alternative filtering schemes and solutions. To this aim, several methods have been proposed for the analysis of transmission line structures illuminated by an EM field with random polarizations and incidence directions [6]–[9]. Also, a number of different approaches and methodologies have been developed to model the electromagnetic interaction of a metal shield with apertures illuminated by an external field [10]–[11]. However, an accurate physically-based model of all the elements involved in the immunity test requires detailed information on both the vehicle structure and the on-board electrical and electronic devices. In addition, possible non-uniformity on the cable geometry or irregularities in the metallic structure must be carefully modeled and taken into account, the consequence being a demanding activity to define the detailed physical description of the system.

This paper proposes a black-box approach for the prediction of the currents induced on a generic linear load during the radiated immunity test. The proposed modeling scheme relies on a parametric Thévenin-based circuit interpretation of the radiated immunity setup which combines the SVM-regression [12]–[13] with an adaptive algorithm. The latter allows generating an accurate model of the equivalent voltage source from a small set of tabulated frequency-domain data obtained from either full-wave simulations or experimental results, without requiring any knowledge of the geometry of the components and structures of the measurement setup. The obtained model allows estimating the spectrum envelope of the currents induced by the external RF field excitation, for different angular positions of the vehicle [8]. The feasibility and the robustness of the proposed approach are demonstrated based on the results of a set of full-wave simulations by considering a synthetic test structure.

## II. RADIATED IMMUNITY TEST & SIMULATION SETUP

According to the standard [5], the automotive radiated immunity test consists of an EM field impinging the vehicle under test placed on a rotating platform. The aim of the test is to measure frequency-by-frequency the *maximum* level of the noise currents induced on the most relevant on-board electrical and electronic components w.r.t. the considered angular position  $\phi$  of the vehicle. The measurement is accomplished by recording the spectra of the currents induced by an external field in the ECU loads for a set of different angular positions of the vehicle.

R. Trincherò, I. S. Stievano and F. G. Canavero are with the EMC Group, Department of Electronics and Telecommunications, Politecnico di Torino, 10129 Torino, Italy (e-mail: riccardo.trincherò@polito.it, igor.stievano@polito.it, flavio.canavero@polito.it).

For simulation purposes, a simplified version of the automotive immunity test has been implemented in CST MICROWAVE STUDIO. The vehicle is modeled as a perfect electric conductor (PEC) structure of dimension  $3.6\text{ m} \times 1.55\text{ m} \times 2.2\text{ m}$  with four apertures of dimensions  $0.55\text{ m} \times 1.3\text{ m}$  and  $0.38\text{ m} \times 0.95\text{ m}$  representing the front, back and lateral windows (see Fig. 1(a)). A transmission line of length  $L = 1\text{ m}$  is placed inside the vehicle at a fixed height of  $h = 18\text{ cm}$  w.r.t. the vehicle floor, which is represented by a PEC plane. As shown in Fig. 1(b), the transmission line is terminated on one side with a resistive load  $Z_S(\omega) = 1\text{ k}\Omega$  and with a generic lumped load  $Z_L(\omega)$  at the opposite end, the latter impedance representing the equivalent input impedance of the ECU. The vehicle chassis, the transmission line and their coupling with the external field have been simulated via the full-wave solver of CST. The rotation of the vehicle is accounted for by varying the azimuth angle  $\phi$  of the external field excitation impinging the vehicle.

The field excitation consists of a vertically polarized plane wave of amplitude  $1\text{ V/m}$ . The simulation setup allows extracting the spectra of the current  $I_L$  induced on the transmission line ECU termination by an incident wave for  $N_\phi = 150$  different angles  $\phi_i$ , with  $0 \leq \phi_i < 2\pi$ , in the frequency bandwidth  $20\text{ MHz}$  to  $1\text{ GHz}$ <sup>1</sup>, for  $N_f = 124$  frequency samples. The simulation output is a sampled version of the current  $I_L(\omega_k; \phi_i)$ , with  $\omega_k = 2\pi f_k$  for  $f_k \in \mathcal{F} = \{f_1, \dots, f_{N_f}\}$  and  $\phi_i \in \mathcal{A} = \{\phi_1, \dots, \phi_{N_\phi}\}$ . The samples can be used to estimate the maximum induced current spectrum, such as,

$$|I_{L,MAX}(\omega_k)| = \max_{\phi_i \in \mathcal{A}} \{|I_L(\omega_k; \phi_i)|\}. \quad (1)$$

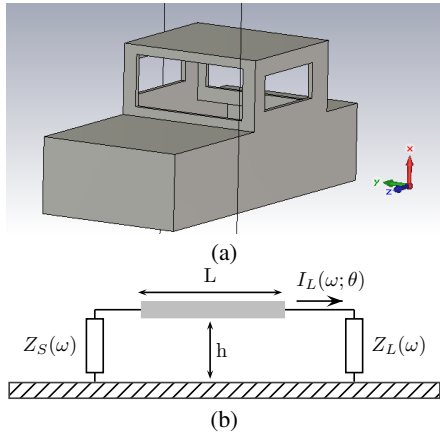


Figure 1: Panel (a): Implementation of the metallic body of the vehicle in CST MICROWAVE STUDIO; Panel (b): transmission line structure placed inside the vehicle with the corresponding parameters and terminations.

### III. THÉVENIN-BASED METAMODEL ESTIMATION

#### A. Thévenin Equivalent: Parameters Estimation

The spectrum of the current  $I_L(\omega; \phi)$  induced by an external field on a generic ECU termination placed inside

the vehicle (see Fig. 2(a)), can be fully captured via the Thévenin equivalent shown in Fig. 2(b). In the above circuit, the source  $V_{eq}(\omega; \phi)$  represents the voltage induced at the ECU port by an external EM field with propagation direction  $\phi$ , when the lumped load  $Z_L(\omega)$  is replaced by an open circuit. On the other hand, the equivalent impedance  $Z_{eq}(\omega)$  is independent from both the direction and the amplitude of the incident field and is defined as the impedance seen by the ECU when the external field is powered off.

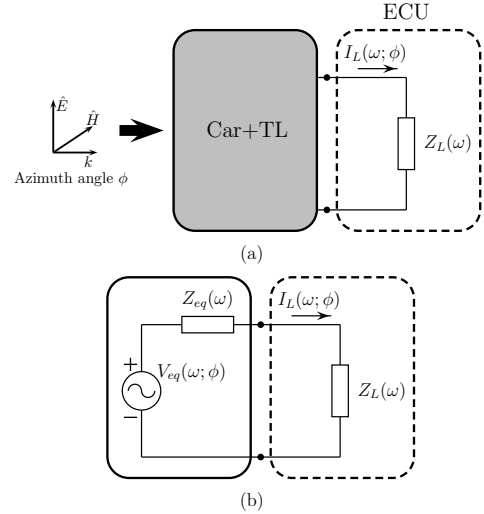


Figure 2: Illustration of the equivalence between the immunity test setup (top panel) and its corresponding Thévenin-based circuit interpretation (bottom panel).

Due to the linearity of the considered car structure, the equivalent impedance  $Z_{eq}$  can be suitably estimated by means of a one-port scattering simulation or measurement. Once the equivalent impedance is known, the amplitude and phase of the equivalent voltage source  $V_{eq}(\omega_k; \phi_i)$ , for an excitation with azimuth angle  $\phi_i \in \mathcal{A}$  at angular frequency  $\omega_k \in \mathcal{F}$ , can be suitably estimated from the current  $I_{L0}(\omega_k; \phi_i)$  flowing through a known load  $Z_L(\omega_k) = Z_{L0}(\omega_k)$ , obtained from either simulations or experimental results, as follows:

$$V_{eq}(\omega_k; \phi_i) = I_{L0}(\omega_k; \phi_i)(Z_{eq}(\omega_k) + Z_{L0}(\omega_k)). \quad (2)$$

From the above equation, the magnitude and phase of current  $I_L(\omega_k; \phi_i)$  for a generic load  $Z_L$  can be suitably estimated, i.e.,  $I_L(\omega_k; \phi_i) = V_{eq}(\omega_k; \phi_i) / (Z_{eq}(\omega_k) + Z_L(\omega_k))$ . The spectrum of the maximum current amplitude induced on a generic impedance  $Z_L$  is then estimated via (1). It is important to remark that the above circuit interpretation can be suitably extended to the case of a linear multiport structure, representing a wire bundle connected to several ECUs inside the car body.

#### B. SVM-Based Metamodel via Adaptive Algorithm

In order to provide a continuous model of the voltage source  $V_{eq}(\omega_k; \phi_i)$ , so that it allows predicting the complex values of the equivalent Thévenin source for any value of the angle  $\phi \in \mathbb{R}$ , the available samples of the voltage source  $V_{eq}(\omega_k; \phi_i)$  can be used as training samples for the SVM regression. The

<sup>1</sup>First portion of the frequency range specified by the standard ISO 11452-2 [5] for the radiated immunity test.

inherent periodic behavior of the Thévenin source w.r.t. the incidence angle  $\phi$  (i.e.,  $V_{eq}(\omega_k; 0) = V_{eq}(\omega_k; 2\pi)$ ) can be properly accounted for by considering a SVM regression with a periodic regularized Fourier kernel, which writes [12],

$$V_{eq, SVM}(\omega_k; \phi) = \sum_{i=1}^{N_\phi} \beta_i(\omega_k) K(\phi_i, \phi) + b(\omega_k), \quad (3)$$

where  $\beta_i(\omega_k)$  are the weight coefficients and  $b(\omega_k)$  is a scalar term providing the offset of the non-linear regression and the kernel  $K(\phi_i, \phi)$  is the periodic regularized Fourier expansion [12], which writes

$$K(\phi_i, \phi) = \frac{1 - q^2}{2(1 - 2q \cos(\phi_i - \phi) + q^2)}, \text{ for } 0 < q \leq 1. \quad (4)$$

For each angular frequency  $\omega_k$ , the parameters  $\beta_i(\omega_k)$  and  $b(\omega_k)$  are estimated via the solution of a convex optimization problem defined by the  $\varepsilon$ -intensive loss function presented in [12]. The SVM-regression has been used to train two different regressions corresponding to the real and the imaginary part of the available realizations of  $V_{eq}$ . It is important to remark that, unlike the standard discrete Fourier transform (DFT), the proposed nonlinear SVM regression with Fourier kernel can be suitably applied to a set of non-uniformly spaced samples.

However, the accuracy of the resulting metamodel  $V_{eq, SVM}$  unavoidably depends on the quality of the samples used to train it. In this specific application, we are looking for the minimum number of training samples  $N_\phi$  for which the maximum values of the  $V_{eq, SVM}$  w.r.t. the angle  $\phi$  is correctly captured by the model. This allows minimizing the number of simulations or measurements needed to build the model, thus minimizing the lab use or the computational costs. Unfortunately, the effect of the number of training samples on the final model accuracy cannot be exactly known a priori, since it depends on the problem complexity.

In order to overcome the above issue, the adaptive algorithm in Alg. 1 has been proposed. Alg. 1 goes as follows: at a given  $j$ -th iteration, the algorithm uses a set of  $N_\phi^j = 2^{(j-1)} N_0$  (i.e.,  $N_\phi^j = 2N_\phi^{(j-1)}$ ) for which the incidence angles  $\mathcal{A}^j = \{\phi_1, \dots, \phi_{N_\phi^j}\}$  are defined as:

$$\phi_i = \phi_0 + \frac{2\pi}{N_\phi^j} (i - 1), \text{ for } i = 1, \dots, N_\phi^j, \quad (5)$$

where  $\phi_0$  is a parameter (i.e.,  $0 \leq \phi_0 < 2\pi$ ) defining the offset angle and  $N_0$  represents the initial number of angles at the first iteration.

It is important to remark that, thanks to the properties of the SVM regression with the Fourier kernel, the proposed algorithm can be applied also to the more general case for which, at each iteration, the new angular samples are randomly selected. The new values in the angular set  $\mathcal{A}^j$  are then used as input parameters for a parametric simulation (or measurement) of the radiated immunity test to compute the corresponding response samples of the current  $I_L(\omega_k; \phi_i)$  for any  $\omega_k \in \mathcal{F}$ . The latter are used as new training samples for generating the metamodel of the Thévenin source  $V_{eq, SVM}(\omega_k; \phi)$  via (3). In

order to monitor the effect of the new current samples on the model accuracy, the resulting metamodel  $V_{eq, SVM}$  is evaluated on a fine grid  $\hat{\mathcal{A}} = \{\hat{\phi}_1, \dots, \hat{\phi}_{\hat{N}_\phi}\}$  with  $\hat{N}_\phi$  uniformly spaced angles, to compute the following maximum and mean value spectra:

$$V_M^j(\omega_k) = \max_{\hat{\phi}_i \in \hat{\mathcal{A}}} \{V_{eq, SVM}^j(\omega_k; \hat{\phi}_i)\}, \quad (6a)$$

$$V_\mu^j(\omega_k) = \frac{1}{\hat{N}_\phi} \sum_{n=1}^{\hat{N}_\phi} V_{eq, SVM}^j(\omega_k; \hat{\phi}_i). \quad (6b)$$

The level of accuracy of the metamodel is then estimated via a weighted linear combination of the relative errors in the  $L_2$ -norm of the spectra in (6) computed at the present iteration w.r.t. their values predicted at the previous iteration, via the following error estimator:

$$\varepsilon = \alpha_M \frac{\|V_M^j(\omega_k) - V_M^{j-1}(\omega_k)\|_2}{\|V_M^j(\omega_k)\|_2} + \alpha_\mu \frac{\|V_\mu^j(\omega_k) - V_\mu^{j-1}(\omega_k)\|_2}{\|V_\mu^j(\omega_k)\|_2}, \quad (7)$$

where  $\alpha_M$  and  $\alpha_\mu$  are the weight coefficients for the relative error of the maximum and the mean value spectra, respectively.

The algorithm ends when  $\varepsilon < tol$ . Until the convergence is reached, the number of training angular samples  $N_\phi^j$  is increased by  $N_\phi^{j-1}$  new samples at each iteration.

---

**Algorithm 1** Adaptive algorithm for the estimation of the Thévenin-based metamodel.

---

- 1: Initialize:  $j = 0$ ;  $V_M^0 = \text{Inf}$ ;  $V_\mu^0 = \text{Inf}$ ;
  - 2: Set parameters:  $N_0$ ;  $\phi_0$ ;  $\hat{N}_\phi$ ;  $\alpha_M$ ;  $\alpha_\mu$ ;  $tol$ ;  $q$ ;
  - 3: **while**  $\varepsilon < tol$  **do**
  - 4:   Do  $j++$ ;
  - 5:   Update  $N_\phi^j$  and compute the angles  $\phi_i \in \mathcal{A}^j$  via (5);
  - 6:   Get the new samples of  $I_L(\omega_k; \phi_i)$
  - 7:   Estimate  $V_{eq}^j(\omega_k; \phi_i)$  and  $Z_{eq}(\omega_k)$  via (2);
  - 8:   Build the metamodel  $V_{eq, SVM}^j(\omega_k; \phi)$  as in (3);
  - 9:   Estimate  $V_{eq, SVM}^j(\omega_k; \hat{\phi}_i)$  for any  $\hat{\phi}_i \in \hat{\mathcal{A}}$ ;
  - 10:   Calculate  $V_M^j$  and  $V_\mu^j$  via (6) and the error  $\varepsilon$  via (7);
  - 11: **end while**
  - 12:  $V_{eq, SVM} = V_{eq, SVM}^j$ ;
- 

#### IV. APPLICATION EXAMPLE: RADIATED IMMUNITY TEST

The proposed modeling procedure is validated by considering the current spectra  $I_L(\omega; \phi)$  and  $I_{L, MAX}(\omega)$  induced on the ECU termination simulated by a load  $Z_L(\omega) = R + j\omega L + 1/j\omega C$ , where  $R = 10 \Omega$ ,  $L = 0.1 \mu\text{H}$  and  $C = 0.1 \text{nF}$  in the frequency bandwidth from 20 MHz to 1 GHz.

The Thévenin-based metamodel has been estimated via the modeling scheme presented in Sec. III. The iterative algorithm Alg. 1 has been run with  $tol = 0.05$ ,  $\alpha_M = \alpha_\mu = 0.5$ ,  $q = 0.5$ ,  $\hat{N}_\phi = 180$  and  $N_0 = 4$ . As a part of the algorithm application, the parameters  $Z_{eq}$  and  $V_{eq}$  are estimated from the one-port scattering parameters and the current samples  $I_{L, 0}(\omega; \phi_i)$  obtained for  $Z_{L0} = 50 \Omega$ , respectively. The algorithm converges after 4 iterations by using a training set with  $N_\phi^4 = 32$  samples, only.

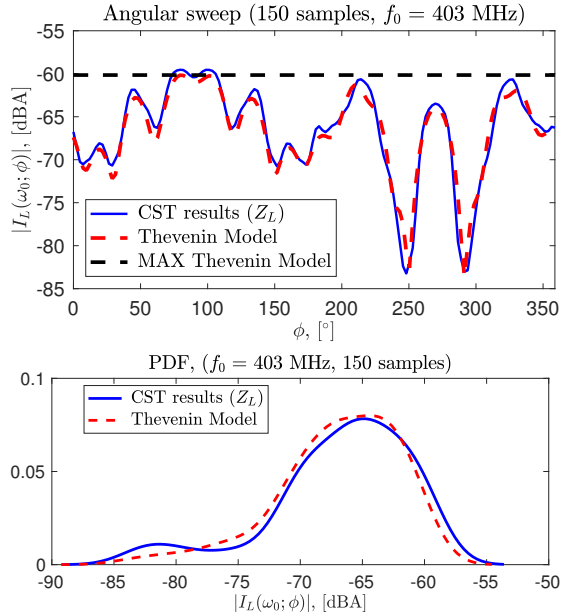


Figure 3: Induced current on the ECU termination for an incidence field at  $f_0 = 403$  MHz as a function of the angle  $\phi$  (top panel) and corresponding PDF (bottom panel), obtained via CST simulations (blue curves) and via the proposed modeling scheme with  $N_\phi^4 = 32$  samples (red curves).

As a first validation, Fig. 3 shows a comparison for the current magnitude  $I_L(2\pi f_0; \phi_i)$  for  $f_0 = 403$  MHz obtained for 150 angular values of  $\phi_i$  (top panel) and the corresponding probability density function (PDF) (bottom panel) provided by a parametric CST simulation with the ones predicted by the proposed Thévenin-based metamodel. The results highlight the capability of the proposed modeling scheme to capture the main features of the angle dependence and of the corresponding PDF, even if a relatively small set of training sample (i.e., 32) is used to generate the metamodel.

As a further validation, Fig. 4 compares the spectra of the maximum and the mean values of the current  $I_L(\omega; \phi)$  estimated by the the metamodel and by 150 full-wave simulations, in the bandwidth from 20 MHz to 1 GHz. The comparison highlights once again the good accuracy – excellent in the low portion of the spectrum – of the proposed metamodel, which allows predicting both the maximum and the mean values of the induced current in the considered bandwidth with an average distance w.r.t. the actual maximum current spectrum of  $\leq 3$  dB. It is also important to remark that after an initial overhead for generating the parametric Thévenin equivalent, the obtained model allows estimating the maximum current spectrum for any linear load in 19 s, while a complete parametric full-wave simulation with 150 angles takes  $\sim 119$  h on a Intel(R) Core(TM) i7-6700M CPU running at 3.40 GHz with 16 GB of RAM.

## V. CONCLUSIONS

This paper proposed a black-box modeling approach for the prediction of the spectrum of the maximum currents induced on a generic linear load, during the radiated immunity test.

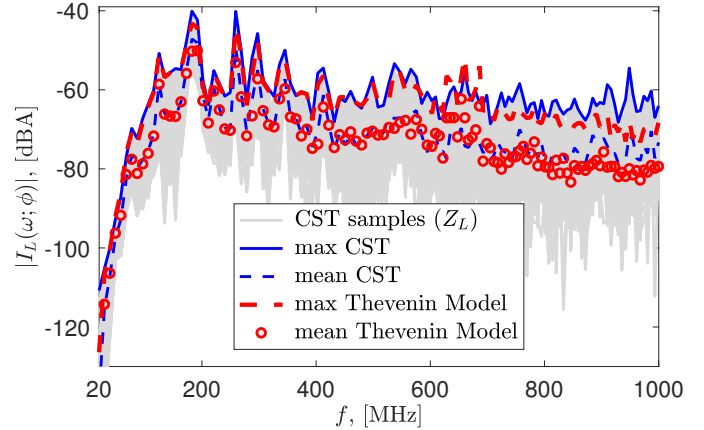


Figure 4: Magnitudes of the current induced in the ECU termination for 150 different incidence angles  $\phi$  (gray curves). The maximum and the mean values of the currents obtained via CST (blue curves and circles) are compared with the maximum values predicted the corresponding metamodel built from  $N_\phi^4 = 32$  samples (red curve and circles).

The proposed modeling strategy relies on a Thévenin-based interpretation of the test setup resulting by combining the SVM regression with an adaptive algorithm. The latter allows defining the minimum number of training samples needed to accurately predict the maximum values of the induced current for different field excitations and load conditions. The metamodel predictions have been compared with the results of 150 deterministic CST simulations.

## REFERENCES

- [1] C. R. Paul, *Introduction to Electromagnetic Compatibility: Second Edition*. John Wiley&Sons, Inc., Hoboken: New Jersey, 2006.
- [2] K. P. Moy, “EMC related issues for power electronics,” *Automotive Power Electronics*, Dearborn, MI, 1989, pp. 46–53.
- [3] H. Rakouth, *et al.*, “Automotive EMC: Key Concepts for Immunity Testing,” in *Proc. IEEE 2007 Int. Symp. on EMC*, Honolulu, HI, 2007.
- [4] A. M. Silaghi, *et al.*, “Measurement of radiated immunity in the automotive industry: Key concepts,” in *Proc. IEEE 12th Int. Symp. on Electronics and Telecommunications*, Timisoara, 2016, pp. 25–28.
- [5] Road Vehicles & Component Test Methods for Electrical Disturbances From Narrowband Radiated Electromagnetic Energy—Part 4: Harness Excitation Methods, ISO 11452-4, Dec. 2011.
- [6] F. Grassi, G. Spadacini, and S. A. Pignari, “The concept of weak imbalance and its role in the emissions and immunity of differential lines,” *IEEE Trans. Electromagn. Compat.*, Vol. 55, No. 6, pp. 1346–1349, Dec. 2013.
- [7] I. Junqua, J. Parmantier and P. Degauque, “Field-to-Wire Coupling in an Electrically Large Cavity: A Semianalytic Solution,” *Trans. on Electromagn. Compat.* Vol. 52, No. 4, pp. 1034–1040, Nov. 2010.
- [8] S. Grivet-Talocia and E. Fevola, “Compact Parameterized Black-Box Modeling via Fourier-Rational Approximations,” *IEEE Trans. Electromagn. Compat.*, Vol. 59, No. 4, pp. 1133–1142, Aug. 2017.
- [9] P. Manfredi and F. G. Canavero, “Polynomial Chaos for Random Field Coupling to Transmission Lines,” *Trans. on Electromagn. Compat.*, Vol. 54, No. 3, pp. 677–680, June 2012.
- [10] A. J. McDowell and T. H. Hubing, “Analysis and Comparison of Plane Wave Shielding Effectiveness Decompositions,” *Trans. on Electromagn. Compat.*, Vol. 56, No. 6, pp. 1711–1714, Dec. 2014.
- [11] E. Liu, *et al.*, “Accuracy Analysis of Shielding Effectiveness of Enclosures With Apertures: A Parametric Study,” *Trans. on Electromagn. Compat.*, Vol. 56, No. 6, pp. 1396–1403, Dec. 2014.
- [12] V. Vapnik, *Statistical Learning Theory*, John Wiley and Sons, NY, 1998.
- [13] R. Trincherro, *et al.*, “Machine Learning for the Performance Assessment of High-Speed Links”, *Trans. Electromagn. Compat.*, Vol. 60, No. 6, pp. 1627–1634, Dec. 2018.